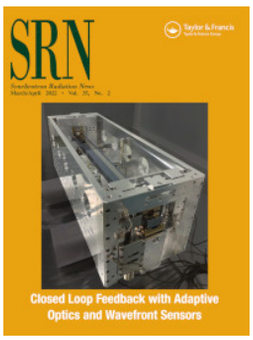


Synchrotron Radiation News

ISSN: (Print) (Online) Journal homepage: https://www.tandfonline.com/loi/gsrn20

# The Versatile Soft X-ray (VerSoX) Beamline at Diamond Light Source

David C. Grinter, Federica Venturini, Pilar Ferrer, Matthijs A. van Spronsen, Rosa Arrigo, Wilson Quevedo Garzon, Kanak Roy, Alexander I. Large, Santosh Kumar & Georg Held

**To cite this article:** David C. Grinter, Federica Venturini, Pilar Ferrer, Matthijs A. van Spronsen, Rosa Arrigo, Wilson Quevedo Garzon, Kanak Roy, Alexander I. Large, Santosh Kumar & Georg Held (2022): The Versatile Soft X-ray (VerSoX) Beamline at Diamond Light Source, Synchrotron Radiation News, DOI: 10.1080/08940886.2022.2082181

**To link to this article:** https://doi.org/10.1080/08940886.2022.2082181



Published online: 01 Jul 2022.

OPEN ACCESS

TECHNICAL REPORT

# The Versatile Soft X-ray (VerSoX) Beamline at Diamond Light Source

David C. Grinter,[1] Federica Venturini,[1] Pilar Ferrer,[1] Matthijs A. van Spronsen,[1] Rosa Arrigo,[1,2] Wilson Quevedo Garzon,[1,3] Kanak Roy,[1] Alexander I. Large,[1] Santosh Kumar,[1] and Georg Held[1]

[1]*Diamond Light Source Ltd, Oxfordshire, UK*

[2]*School of Science, Engineering and Environment, University of Salford, Manchester, UK*

[3]*Helmholtz-Zentrum Berlin für Materialien und Energie, Berlin, Germany*

*Georg Held* *georg.held@diamond.ac.uk*

## Introduction

Over the last few decades, there has been growing demand for a better understanding of the near-surface regions of a variety of samples in non-vacuum environments [1, 2], including heterogeneous catalysts under reaction conditions, electrochemical interfaces, pharmaceuticals and biomaterials in aqueous environments, electronic and photonic devices under realistic humidity conditions, and environmental studies on liquids and ices. All of these areas of science have a common interest in the chemical nature and composition of the near-surface region within a few nm. This is best characterized using soft or tender X-ray techniques, such as photoelectron spectroscopy (XPS) and near-edge X-ray absorption fine structure (NEXAFS) spectroscopy.

Efforts to design and build instruments enabling the study of such systems, both at synchrotrons and in the laboratory, have been described by a number of authors in recent publications [3–19]. The Versatile Soft X-ray (VerSoX) beamline B07 of Diamond Light Source consists of two branches, B and C, which can be operated simultaneously and independently in the energy range 45–2200 eV and 130–2800 eV, respectively. Branch C was completed in July 2017 [20]. It features a near ambient-pressure end station capable of performing XPS (X-ray photoelectron Spectroscopy) and NEXAFS (Near-edge X-ray absorption fine structure) spectroscopy experiments at gas pressures up to tens of mbar. Branch B was completed in May 2021. It currently features an end station dedicated to high-throughput NEXAFS experiments capable of reaching pressure in the 1000 mbar range; a second endstation enabling high-throughput ultra-high vacuum UHV experiments is currently being commissioned. Ultimately, the combination of the two branches spans the pressure range between ultra-high vacuum and several bar, and thus offers a bridge over the pressure gap.

The beamline enables studying the surface composition of heterogeneous catalysts under working conditions (as opposed to conventional *ex situ* characterization), characterization of biological and pharmaceutical samples under equilibrium water-vapor pressures, and direct spectroscopy of solid-liquid interfaces, which are key to electrochemical applications. It also allows studies of samples, such as those related to battery research, heritage conservation, and new functional materials (MOFs, polymers, etc.), which usually do not require high ambient pressures but are still often incompatible with ultra-high vacuum requirements due to outgassing. Automated sample manipulation for high throughput is a key feature of Branch B and is continuously improved in ongoing upgrades. Another scientific aim of the beamline is to facilitate the development of new or less common detection techniques for soft X-ray absorption spectroscopy, such as X-ray fluorescence or optical luminescence, and reaction cells for even more challenging sample environments (e.g. batteries, electrochemical cells, etc.) than those already available.

In this article, we present the design of the beamline and endstations, their performance, and a small selection of data demonstrating the capabilities of the instrument. Additional examples of data recorded with the instrument can be found in [20] and in the publications listed in the Summary section.

## Beamline

The beamline B07 consists of two branchlines, B and C, each of which has its own source and monochromator. Therefore, they can be operated simultaneously and independently (see Figure 1). The optical design of the two branches is very similar; however, the energy ranges differ somewhat in order to suit each branch's requirements. XPS at pressures above 5 mbar and at the solid-liquid interface requires high photon energies [20]. Therefore, the energy range of branch C was extended as far as possible at the upper end, covering 130–2800 eV. The range of branch B is 45 eV to 2200 eV, which covers the Li K-edge and the $N_{6,7}$ absorption edges of the sixth row Pt group metals.

The overall design criterion for both branches was to get maximum possible photon flux and reasonable energy resolution ($E/\Delta E > 5000$) over a wide range of photon energies. Figure 1(a) shows an overview of the beamline design. The source is a 1.4 T bending magnet emitting horizontally polarized radiation spread horizontally over approximately 30 mrad. Two segments of this fan, at around 7 mrad and 23 mrad, are reflected into the two branchlines B and C by a pair of mirrors, M1b and M1c, respectively, at distances 13.2 and 13.1 m from the bending magnet source. The acceptance angles of these mirrors (2.0/2.4 mrad horizontal and 0.4 mrad vertical) limit the photon flux into the monochromators to values between $1 \times 10^{13}$ and $3 \times 10^{13}$ ph (s 0.1% BW)$^{-1}$ over

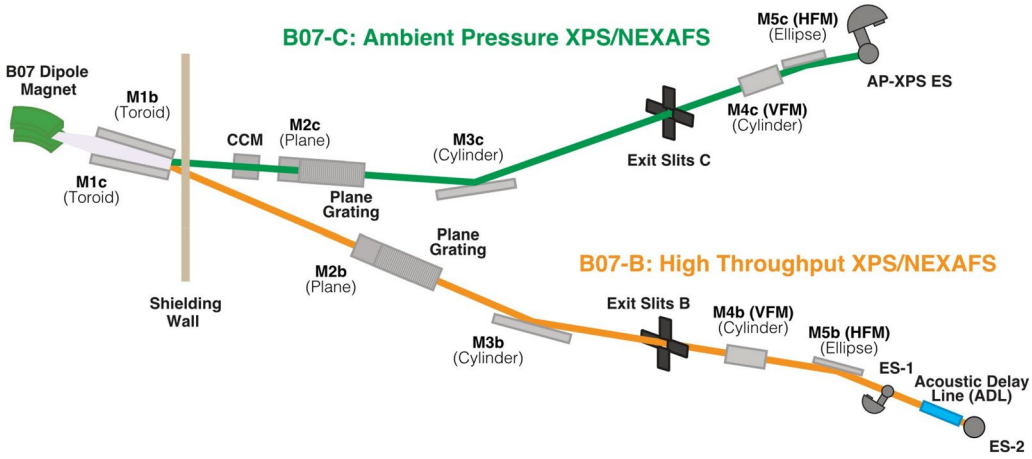


*Figure 1*: *General layout of the beamline including both branchlines B and C.*

the respective energy ranges at 300 mA ring current. The M1 mirrors are toroids that collimate the beam in vertical direction and focus horizontally onto the exit slit of their collimated Plane Grating Monochromator type [21] (cPGM, manufactured by FMB Berlin). M3b/c focus the monochromatic beam vertically onto the exit slits located 8.5 m and 7.5 m, respectively, downstream. Each cPGM has three gratings with 400, 600, and 1000 /1200 lines $mm^{-1}$, designed to provide an energy resolving power $h\nu/\Delta(h\nu) > 5000$ over most of the energy range. The use of incident collimated light allows working with variable $c_{ff}$ and thus optimizing the suppression of second and higher diffraction orders. As an alternative to the cPGM, branch C also has three channel-cut Si crystal monochromators [22], which can be inserted into the beamline before the cPGM, bypassing M2c while the gratings are retracted from the path of the synchrotron radiation. These provide fixed- energy monochromatic radiation of 2000, 2250, and 2500 eV with higher resolution and flux than the cPGM at these energies. A pair of refocusing mirrors, M4b/c (vertical) and M5b/c (horizontal), located after the exit slit, focus the monochromatic beam onto the sample position. Branch B has two pairs of refocusing mirrors that provide two foci for two endstations, 2.0 m apart. All motions of optical elements, shutters, diagnostics, and vacuum control are fully integrated in the EPICS (Experimental Physics and Industrial Control System and GDA (Generic Data Acquisition) control environment of the beamline [23, 24].

The beam sizes at the sample positions were measured to be 120 µm (H) × 40–120 µm (V) for Branch B at the second focus (using a calibrated camera) and 90 $\mu$m (H) × 60-100 $\mu$m (V) for Branch C (using a thin mica sheet). For both branches, the vertical height depends on the opening of the exit slit. Figure 2 shows the transmission and energy resolution (extrapolated from gas absorption data using the formulae provided in ref. [21]) of both branchlines for the different gratings. Branch B achieves better energy resolution than C, which is due to a combination of smaller distortion of M1b compared to M1c and a smaller minimum exit slit opening of 0.005 mm versus 0.012 mm.

A key improvement in the vacuum design of the beamline is that all optical elements are operated in an atmosphere of 1–2 × $10^{-8}$ mbar oxygen (controlled via leak valves), which is approximately one order of magnitude higher than the base pressure of the vacuum vessels. Oxygen is activated by the incident X-rays near the mirror surfaces and reacts with carbon to form volatile compounds, CO or $CO_2$, thus avoiding the build-up of carbon deposits [20, 25]. In this way, features due to carbon K-edge absorption around 285 eV, which are very prominent in most other soft X-ray beamlines, are reduced to around 10%.

## Endstations

Branch C has one and Branch B two optical foci for endstations, which are also indicated in Figure 1. The near-ambient-pressure (NAP) XPS/NEXAFS endstation is located at the focus of Branch C, which has been operational since July 2017. Branch B features a UHV XPS/NEXAFS end station (ES-1), which is currently being commissioned, and a high-throughput NEXAFS endstation (ES-2), operational since May 2021. Figure 3 shows schematic drawings of all three endstations. In this article, we will concentrate on the NAP endstation of Branch C and ES-2 of Branch B.

*Near-ambient-pressure (NAP) XPS/NEXAFS endstation (Branch C)*

The NAP endstation consists of a differentially pumped beamline entrance and a differentially pumped hemispherical analyzer, which both meet in a single interface flange. The sample chamber is attached to the front of the interface flange, thus allowing the exchange of sample environments while preserving the alignment between beamline and analyzer.

The differentially pumped beamline entrance has four pumping stages. The last aperture (nearest to the sample) has a diameter of 0.3 mm. It is mounted on a nozzle protruding into the interface flange, at around 20 mm from the sample position. All apertures are electrically isolated, such that their drain current can be measured for alignment and

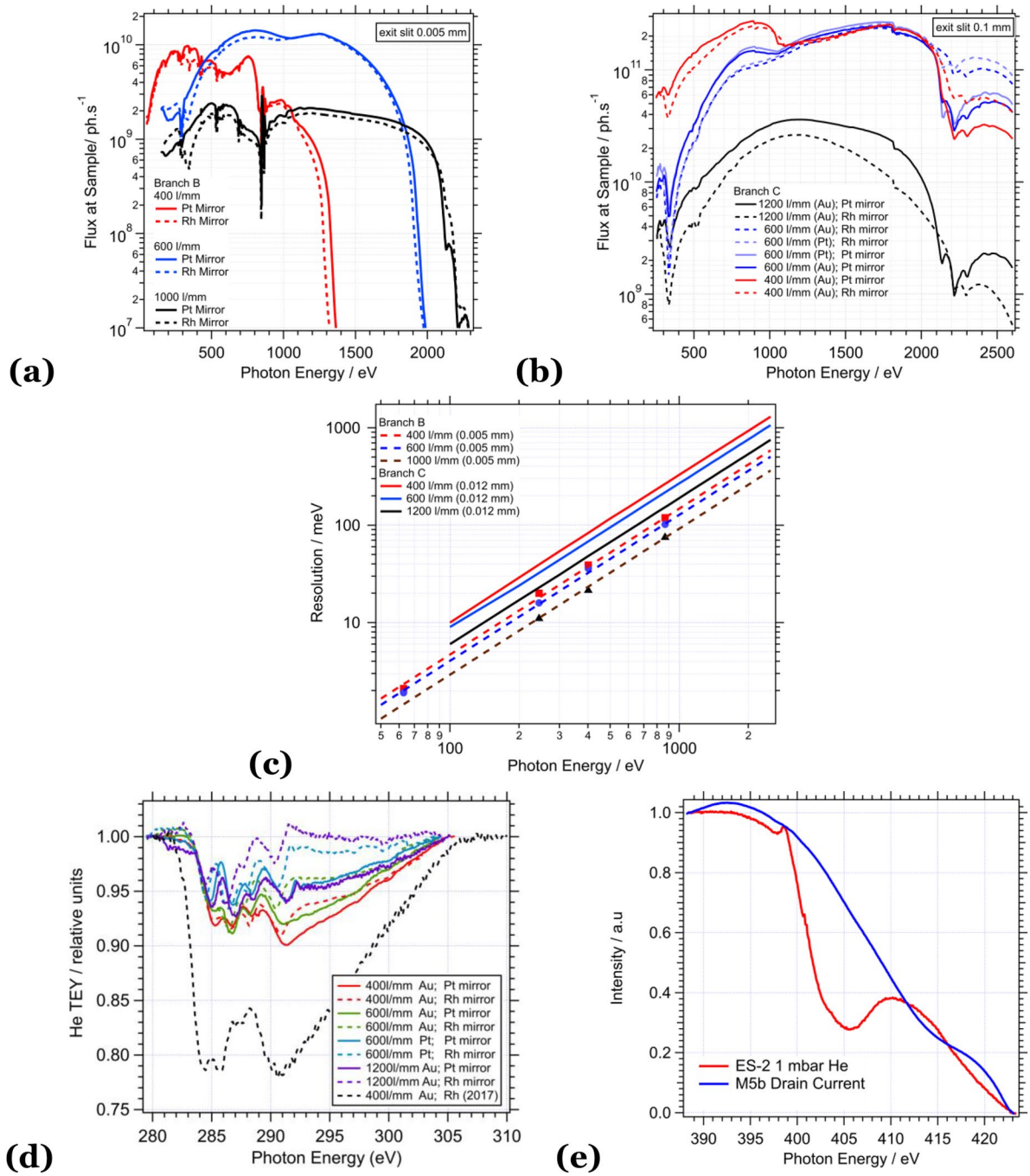


*Figure 2: Transmission of branchline B (a) and C (b) for all combinations of PGM mirrors and gratings; the photon flux was measured using a calibrated photodiode at the sample position. (c) Best achievable resolution (exit slit openings of 0.005 mm and 0.012 mm, respectively) of both branchlines; the plots are based on gas-phase X-ray absorption data (shown for branch B) and extrapolated according to [21]. (d) Transmission of branchline C in the energy range of the carbon K-edge (TEY from He gas in the endstation). (e) Comparison of TEY from the last mirror (M5b, before silicon nitride window) and He gas in ES-2 of branch B (after silicon nitride window).*

calibration purposes. This feature also allows using the last aperture as a total yield detector for gas-phase X-ray absorption spectroscopy. Tests with He gas confirmed that a pressure in the $10^{-9}$ range can be maintained in the last mirror vessel (M5c) while the pressure at the sample is 100 mbar. An array of diagnostics tools is available before the first aperture, near mirror M5c, including a gold mesh (61% transparency)

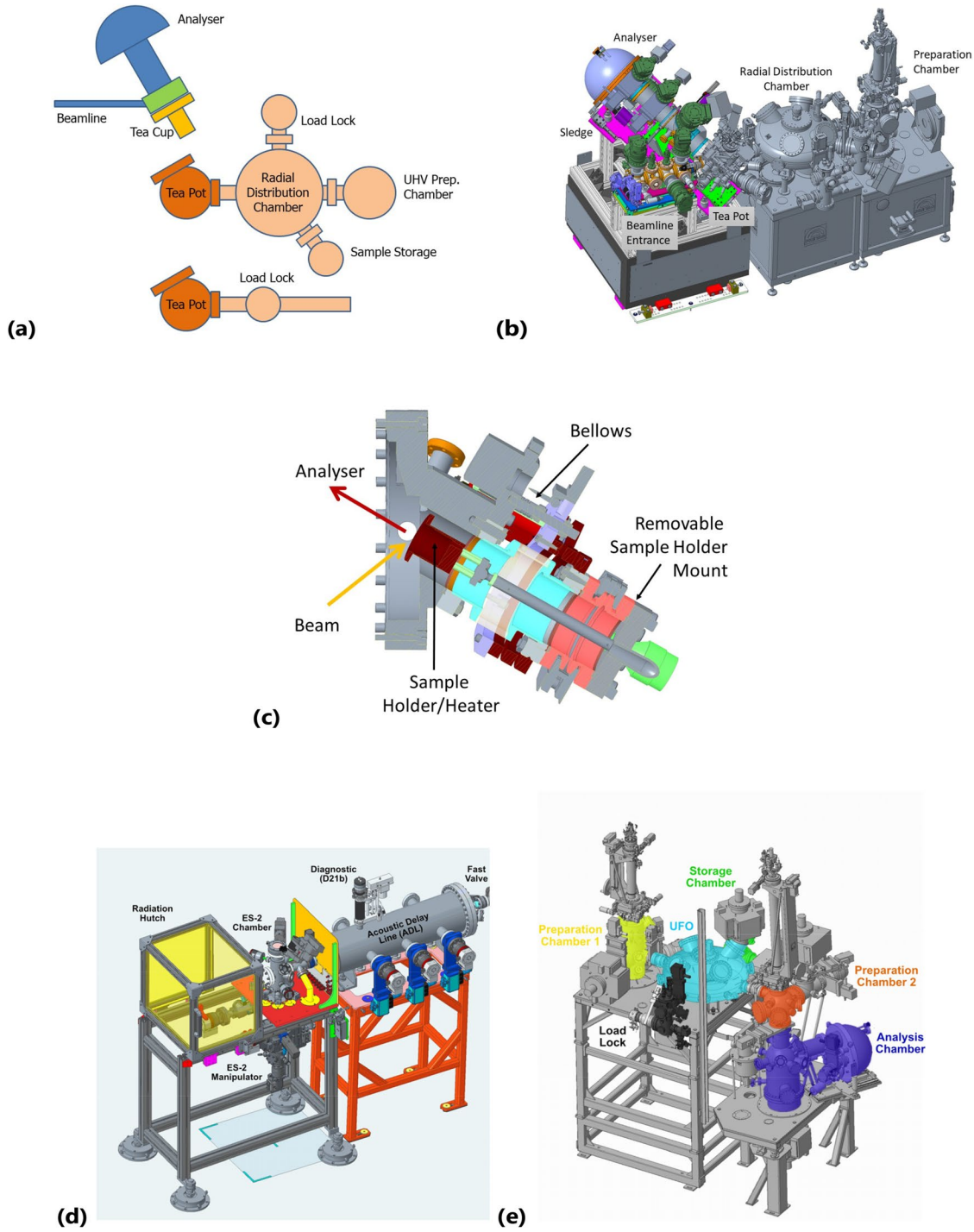


*Figure 3: Overview of the endstations available at VerSoX: (a) schematic arrangement of analyzer, beam- line entrance, and endstations on Branch C; (b) Branch C beamline entrance, analyzer, Tea Pot sample chamber, radial distribution chamber, and preparation chamber; (c) Branch C Tea Cup sample chamber; (d) Branch B ES-2 with acoustic delay line; (e) Branch B ES-1 including analysis chamber, radial distribution chamber ("UFO"), load lock, storage chamber, and two preparation chambers (available in autumn 2022).*

and a photo diode for $I_0$ measurements, and a screen for beam shape diagnostics.

The electron energy analyzer (SPECS PHOIBOS 150 NAP [5]) is mounted at 60° off the synchrotron beam. It is fitted with a prelens, which is also the first of four differential pumping stages, and a 2D delay-line (Surface Concept). The entry cone of the prelens is integrated in the aforementioned interface flange. It can be biased (typically +5 to +36 V) to pull electrons into the analyzer, which leads to about 10% increase in the signal without affecting the measured kinetic energy, and it can be used (simultaneously if required) as electron collector for X-ray absorption measurements or for other purposes. The cone aperture of 0.3 mm diameter is slightly larger than the footprint of the beam at normal emission (≈ 0.2 mm) and allows pressures up to 100 mbar in the analysis chamber while keeping the pressure in the detector section of the analyzer below $10^{-6}$ mbar. The first two differential pumping stages each contain a quadrupole mass spectrometer for the analysis of the sample environment. The working distance between cone and sample is typically around 0.3 mm, which allows detecting photoelectrons (> 1% of vacuum signal) in gas pressures up to about 30 mbar for most gases and 50 mbar in hydrogen. A series of pressure-dependent measurements in nitrogen gas is shown in Figure 4(a). Spectra can be recorded either in scanned or snapshot mode. The latter allows data acquisition times of a few seconds but limits the energy range of spectra to 12% of the pass energy; that is, typically to less than 10 eV. The rate at which scanned spectra can be recorded depends on energy range and pass energy. Typically, 20–40 s per spectrum can be achieved.

The design of the interface flange allows exchanging sample chambers without having to re-adjust the alignment between beamline and analyzer. Currently, the endstation offers two different sample environments, a UHV-compatible chamber with sample transfer system ("Tea Pot") and a smaller reaction cell with fast entry system ("Tea Cup"). The different configurations are schematically depicted in Figure 3(a).

The Tea Pot sample analyzer chamber is fitted with a 5-axis manipulator and sample receiver. Base pressures of $10^{-9}$ mbar are typically reached after a short bakeout. Samples can be heated up to 900 K (depending on gas and pressure) and, if necessary, cooled by liquid nitrogen down to a temperature of 150 K. The sample receivers ("PTS" type by Prevac) have integrated resistive heaters, K-type thermocouples, and spare electrical contacts allowing, e.g., biasing the sample. In its simplest configuration, the Tea Pot consists of the analyzer chamber and an entry lock, which is directly attached (see Figure 3(a), bottom). This setup is best suited for samples that can be prepared *ex situ*; the only treatment *in situ* is through heating and ambient gases. Figure 3(b) depicts an extended configuration where the Tea Pot analyzer chamber is connected to a radial distribution chamber. This enables *in vacuo* transfer of samples between the vacuum load lock, an ultra-high vacuum (UHV) sample storage chamber, a UHV sample preparation chamber, and the analyzer chamber. The UHV preparation chamber is equipped with a sputter gun, a LEED system, two leak valves for gas dosing and provides flanges for up to three evaporator sources. This setup allows treating one sample in the UHV preparation chamber while experiments are performed with another sample in the analyzer chamber. Alternatively, the preparation chamber and transfer system can also be operated off-line and the sample can be transferred via a vacuum suitcase and the entry lock.

The Tea Cup reaction chamber (top of Figure 3(a) and (c)) is mainly dedicated to experiments with powder catalyst samples in reactive and contaminating gas environments at pressures > 0.1 mbar. The over-

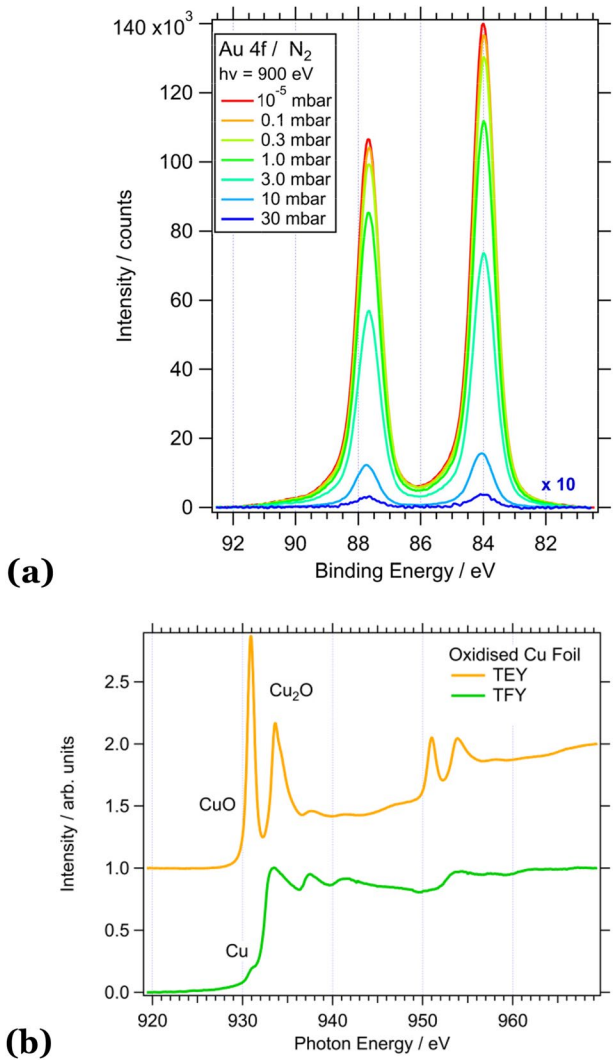


*Figure 4: (a) Au 4f spectra recorded in the NAP endstation at different $N_2$ pressures between $10^{-5}$ and 30 mbar (photon energy = 900 eV); the 30 mbar spectrum is multiplied by factor 10. (b) Cu $L_{2,3}$ NEXAFS spectrum of a copper foil recorded in the ES-2 endstation in electron yield (TEY) and total fluorescence yield (TFY) detection modes.*

arching design principle was to keep the vessel volume small (0.7 L) in order to enable fast switching of environment gases. The sample holder includes a button heater and temperature sensor (Heatwave Labs, max. temperature 700°C). It is mounted on a small manipulator, which allows linear travel along the analyzer axis and tilting in the two directions perpendicular to the analyzer axis, which enables lateral displacements of ±1 mm with negligible change in distance from the analyzer. The Tea Pot chamber also provides easy access for a variety of cells, ranging from high-pressure to electrochemical applications.

A key feature of the NAP endstation is its fully computer-controlled gas delivery system, which can be used for both chambers. It allows controlling the mass flow of up to 14 gases ($H_2$, $CH_4$, $O_2$, $N_2$, $CO_2$, Ar, He, NO, $H_2S$, $NH_3$, CO, plus three spare gases) and also controls the pumping speed of the endstation via a butterfly valve. In this way, both the gas composition (via mass flow ratio) and the gas pressure (via pumping speed) can be controlled separately. The range of gas compositions is approximately 1:100; it is limited by the range of the mass flow controllers (Alicat MC and MCS Series) but can be expanded by using pre-mixed gases. The gases can be admitted to one of two gas lines, which are connected to a switching valve near the endstation. Through this valve, either one of the two gas lines or both can be connected to the endstation. The pressure in the endstation can be controlled by the system between around 0.05 and 30 mbar (depending on gas type). Figure 5(b) shows the user interface of the gas delivery system.

*High-throughput NEXAFS (Branch B)*

Endstation 2 (ES-2) is designed for fast NEXAFS measurements of solid, liquid, and gaseous samples at pressures between $1 \times 10^{-7}$ and 1000 mbar. It is located at the end of the branch line B. Synchrotron radiation passes through endstation 1 (ES-1) and an acoustic delay line (ADL) chamber, as shown in Figure 3(c), before it reaches ES-2. The ambient-pressure chamber is separated from the UHV part of the beamline by a silicon nitride membrane (50–100 nm thick). A fast valve between the acoustic delay line and ES-1 protects the beamline vacuum in case the membrane fails.

NEXAFS spectra can be recorded in total electron yield (TEY) or total fluo- rescence yield (TFY) mode. The former signal is either detected via the sample drain current (for conducting samples) or a positively biased (typically +100 V) ring electrode between sample and beamline window (for insulating samples). For TFY measurements, a photodiode (AXUV 100 G) is used, which is located behind a grounded thin aluminum foil to block photoelectrons and stray visible light. The incoming photon flux, $I_0$, is measured simultaneously with any NEXAFS data at the final refocusing mirror (M5b) using a biased (+36 V) collector plate opposite the mirror surface. In order to correct for any absorption by the silicon nitride window, the chamber is routinely backfilled with a few mbar He and the current on the ring electrode is measured over the absorption edge of interest with the sample out of the beam. The effect of the silicon nitride membrane is shown in Figure 2(e). In this figure, the nitrogen K edge shows only minor variations in the mirror drain current (blue line), whereas the He TEY signal from ES-2 shows a clear dip from the silicon nitride (note the small feature at 400.8 eV is from $N_2$ impurities in the He gas).

Samples are introduced via a fast entry door on the top of the chamber, and mounted either directly on flag-style sample plates or on custom-made multi-sample holders, capable of holding up to 20 samples of $5 \times 5$ mm$^2$. The sample plates fit onto the 4-axis sample manipulator, which can be heated to 400°C in UHV or 200°C in 1 bar (gas dependent). They can be adapted to hold battery cells or cells for *operando* high-pressure (up to several bar) or electrochemical studies.

Figure 4(b) shows data from an oxidized Cu foil. The differences between TEY, which is surface-sensitive and shows predominantly characteristics of CuO and $Cu_2O$, and TFY, which is bulk-sensitive and shows predominantly metallic Cu (for reference see [26, 27], clearly demonstrates the advantages of measuring both signals simultaneously. NEXAFS measurements typically take 0.5 s per data point when one includes the time it takes for the monochromator to move. Thus, a medium resolution spectrum (40 eV range, 0.1 eV steps) can be measured in approximately 200 s.

Inert and non-toxic gases are supplied via manual leak valves and toxic or flammable gases via a mobile gas delivery system that can be connected to the beamline's exhaust system and is equipped with mass flow controllers and full software control, similar to that of the ambient-pressure XPS/NEXAFS endstation. To enable transfer of samples under inert conditions, a vacuum suitcase has been developed that is compatible with most commercial glove boxes, and can be adapted to suit other vacuum systems that use similar flag-style sample plates.

## Computer control, remote operation

All motors (e.g. beamline mirror motion, PGM, manipulators), detectors (e.g., beamline diagnostics, cameras, current amplifiers, electron energy analyzers, mass spectrometers), and sample environment parameters (e.g. temperature, gas pressure/composition) are fully integrated and controlled by the open-source EPICS (Experimental Physics and Industrial Control System) and GDA (Generic Data Acquisition) controls and data acquisition software suite [23, 24]. This enables control of all experimental parameters from the same user interface and thus easy remote access for beamline experiments. The control software consists of three layers:

- Low-level instruments, such as vacuum gauges, pumps, valves, etc., and all safety-relevant systems are operated through programmable logic controllers (PLC).
- All PLCs and high-level instruments (e.g. spectrometers, current amplifiers, motor controllers) are controlled by EPICS drivers, most of which can be directly accessed through graphical user interfaces and instrument windows. Figure 5(a)–(c) show examples of EPICS windows for the Branch C beamline vacuum, the gas rig of the ambient-pressure XPS/NEXAFS endstation, and PGMc, respectively.

- GDA is a scripting environment sitting on top of the EPICS layer, which is used for creating graphical user interfaces for carrying out and monitoring standard exper- iments (e.g. XPS, NEXAFS) but also enables very versatile scripting (in Python) of more complex experimental procedures, such as programmed variation of sample temperature, gas pressure, sample position, and so on.

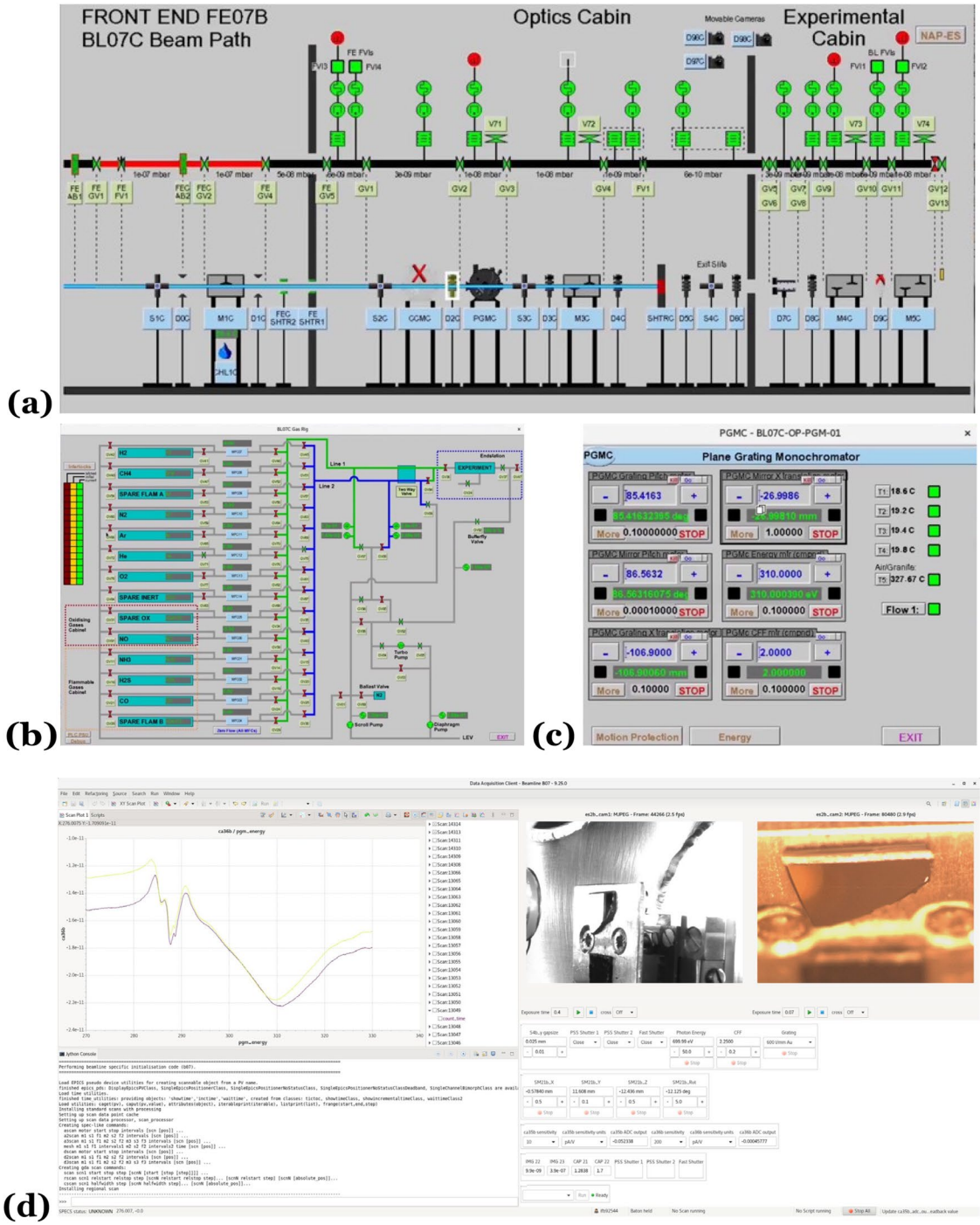


*Figure 5: (a)–(c) Examples of typical EPICS windows of Branch C: (a) vacuum schematic; (b) gas delivery system; (c) PGM; (d) GDA graphical user interface for NEXAFS (Branch B, ES-2).*

This greatly improves the throughput of measurements by permitting the pre-configuration of different absorption edge or core level scans across multiple sample positions that can subsequently be run with minimal user interaction required. The example in Figure 5(d) is the graphical user interface for NEXAFS experiments at ES-2 integrating the live data acquisition display, camera views of the sample from two different angles, and controls for beamline and detector settings.

During beamtime allocations, users are granted remote access to the beamline workstation and have full access to all EPICS and GDA functionalities. This way, the majority of experimental procedures can be executed remotely. The main exceptions are manual sample changes and dosing of gases or liquid vapors, which are not provided by the gas rigs. Also, most user support and troubleshooting can be carried out by beamline staff via remote access, which was of particular advantage during COVID-19 work restrictions that limited the numbers of users and staff allowed on site during experiments.

## Summary and outlook

The two branches of the VerSoX (Versatile Soft X-ray) beamline B07 of Diamond Light Source cover an energy range from 45 eV (minimum energy of branch B) to 2800 eV (maximum energy of branch C) and currently provide endstations for near-ambient-pressure XPS/NEXAFS ($10^{-9}$ to ≈ 30 mbar) ambient-pressure NEXAFS ($10^{-7}$ to ≈ 1000 mbar). The photon flux (typically > $10^{10}$ ph $s^{-1}$ and energy resolution (max. resolving power > 5000 for most of the energy range) is suitable for experiments studying the near-surface chemical composition of functional materials under realistic environmental conditions. Recent experiments carried out at the beamline include near-ambient pressure studies of single crystals [28, 29], model and industrial catalysts [30–33], CVD growth processes [34], solid-liquid interfaces [29], and ionic liquids [35, 36].

In its final stage, when the UHV XPS/NEXAFS endstation ES-1 is operational and various cell designs become available for a wider user community, the VerSoX facility will enable users to bridge the pressure gap and study the same samples under well-controlled UHV conditions all the way up to atmospheric pressures and/or liquid environments. Plans for improvements concurrent with the upgrade of Diamond to a low emittance facility [37] include extending the energy range to tender X-rays (4000 eV) and increasing the flux by installing an undulator source, which will allow faster data acquisition, the study of dilute systems, and denser gas-phase and liquid environments.

## Acknowledgments

We wish to thank Diamond Light Source and its stakeholders for sponsoring this project. Special thanks go to T. Rayment, L. Chapon, C. Nicklin, and the main proposers of the VerSoX beamline, A. Evans and S. L. M. Schröder, for paving the way for this project and contributing significantly to its conceptual design. The authors would also like to extend their thanks to the senior management and support groups of Diamond Light Source for all their contributions, in particular A. Watts, M. Hillman, S. Scott, C. Stephens, C. Green, D. McCue, D. Sheehan, P. Sipos, W. Tizzano, J. Grinrod (mechanical design and installation); M. Hand, A. Walters, H. Wang (optics design); G. Wilkin, S. Patel, P. Larkin, M. Matthews, M. Hilliard, C. Callaway, F. Vulturu, C. Reed (electrical design and installation); L. Pratt, J. J. Mudd, X. Tran, B. Nutter, A. Watson, M. Heath, P. Leicester, S. Lay, P. Amos, A. Grear, J. O'Hea, E. Warwick (control software); T. Richardson, F. Yuan, D. Ladakis, A. Iordachescu, O. King (data acquisition software); H. Shiers, N. Warner, S. Omolayo, M. Duignan (vacuum); and H. Hussain (beamline commissioning). We also acknowledge the fruitful discussions with the suppliers of the main components, FMB Berlin (PGM), Prevac (vacuum systems), and SPECS (electron analyzers). ■

## References

1. M. Salmeron and R. Schlögl, *Surf. Sci. Reports* **63** (4), 169 (2008). doi:10.1016/j.surfrep.2008.01.001
2. D. E. Starr et al., *Chem. Soc. Rev.* **42** (13), 5833 (2013). doi:10.1039/c3cs60057b
3. D. F. Ogletree et al., *Rev. Sci. Instr.* **73** (11), 3872 (2002). doi:10.1063/1.1512336
4. H. Bluhm et al., *J. Electron. Spectrosc. Relat. Phenom.* **150** (2-3), 86 (2006). doi:10.1557/mrs2007.211
5. H. Bluhm et al., *MRS Bull.* **32** (12), 1022 (2007). doi:10.1557/mrs2007.211
6. D. F. Ogletree et al., *Nucl. Instrum. Methods Phys. Res. A* **601**, 151 (2009). doi:10.1016/j.nima.2008.12.155
7. M. E. Grass et al., *Rev. Sci. Instrum.* **81** (5), 053106 (2010). doi:10.1063/1.3427218
8. H. Bluhm, *J. Electron. Spectrosc. Relat. Phenom.* **177** (2-3), 71 (2010). doi:10.1016/j.elspec.2009.08.006
9. J. Schnadt et al., *J. Synchrotron Rad.* **19** (5), 701 (2012). doi:10.1107/S0909049512032700
10. M. A. Brown et al., *Rev. Sci. Instr.* **84** (7), 073904 (2013). doi:10.1063/1.4812786
11. E. J. Crumlin *et al.*, *J. Electron. Spectrosc. Relat. Phenom.* **190**, 84 (2013). doi:10.1016/j.elspec.2013.03.002
12. S. K. Eriksson *et al.*, *Rev. Sci. Instrum.* **85** (7), 075119 (2014). doi:10.1063/1.4890665
13. J. M. Kahk et al., *J. Electron. Spectrosc. Relat. Phenom.* **205**, 57 (2015). doi:10.1016/j.elspec.2015.08.005
14. M. O. Edwards et al., *Nucl. Instrum. Methods Phys. Res. A* **785**, 191 (2015). doi:10.1016/j.nima.2015.02.047
15. J. Knudsen et al., *Surf. Sci.* **646**, 160 (2016). doi:10.1016/j.susc.2015.10.038
16. G. Kerherve et al., *Rev. Sci. Instr.* **88** (3), 033102 (2017). doi:10.1063/1.4975096
17. C. Arble et al., *Surf. Sci. Rep.* **73** (2), 37 (2018). doi:10.1016/j.surfrep.2018.02.002
18. J. Cai et al., *Nucl. Sci. Tech.* **30**, 81 (2019). doi:10.1007/s41365-019-0608-0
19. Z. Novotny et al., *Rev. Sci. Instr.* **91** (2), 023103 (2020). doi:10.1063/1.5128600
20. G. Held et al., *J. Synchrotron Rad.* **27** (5), 1153 (2020). doi:10.1107/S1600577520009157
21. R. Follath et al., *Nucl. Instr. Methods Phys. Res. Sect. A* **390** (3), 388 (1997). doi:10.1016/S0168-9002(97)00401-4
22. L. E. Berman et al., *Res. Sect. A* **241** (1), 295 (1985). doi:10.1016/0168-9002(85)90548-0

23. Experimental Physics and Industrial Control System (EPICS). https://epics-controls.org/
24. Generic Data Acquisition (GDA). http://www.opengda.org/
25. P. Risterucci et al., *J. Synchrotron Rad.* **19** (4), 570 (2012). doi:10.1107/S090904951202050X
26. B. Eren et al., *Phys. Chem. Chem. Phys.* **22** (34), 18806 (2020). doi:10.1039/D0CP00347F
27. R. Arrigo et al., *Faraday Discuss,* advanced online article. (2022). doi:10.1039/D1FD00121C
28. A. Resta et al., *J. Phys. Chem. C.* **124** (40), 22192 (2020). doi:10.1021/acs.jpcc.0c07128
29. C. Byrne et al., *J. Phys. D: Appl. Phys.* **54** (19), 194001 (2021). doi:10.1088/1361-6463/abddfb
30. G. Giorgianni et al., *Phys. Chem. Chem. Phys.* **22** (34), 18788 (2020). doi:10.1039/D0CP00622J
31. M. M.-J. Li et al., *Angew. Chem. Int. Ed.* **59** (37), 16039 (2020). doi:10.1002/anie.202000841
32. A. Large et al., *J. Phys. D: Appl. Phys.* **54** (17), 174006 (2021). doi:10.1088/1361-6463/abde67
33. A. Garcia et al., *J. Power Sources* **490** (229487), 1 (2021). doi:10.1016/j.jpowsour.2021.229487
34. Y. Fan et al., *Nanoscale* **12** (43), 22234 (2020). doi:10.1039/D0NR06459A
35. J. Seymour et al., *Faraday Discuss,* advanced online article. (2022). doi:10.1039/D1FD00117E
36. J. Cole et al., *J. Phys. Chem. C.* **125** (41), 22778 (2021). doi:10.1021/acs.jpcc.1c05738 [
37. L. Chapon et al., *Diamond-II Conceptual Design Report*, Didcot (2019). https://www.diamond.ac.uk/dam/jcr:ec67b7e1-fb91-4a65-b1ce-f646490b564d/Diamond-IIConceptualDesignReport.pdf